

R1-Onevision: Advancing Generalized Multimodal Reasoning through Cross-Modal Formalization

Yi Yang^{1*} Xiaoxuan He^{1,2*} Hongkun Pan^{1*} Xiyang Jiang¹ Yan Deng¹ Xingtao Yang¹
 Haoyu Lu³ Dacheng Yin² Fengyun Rao² Minfeng Zhu¹ Bo Zhang¹ Wei Chen¹
¹ Zhejiang University ² WeChat Vision, Tencent Inc. ³ Renmin University of China

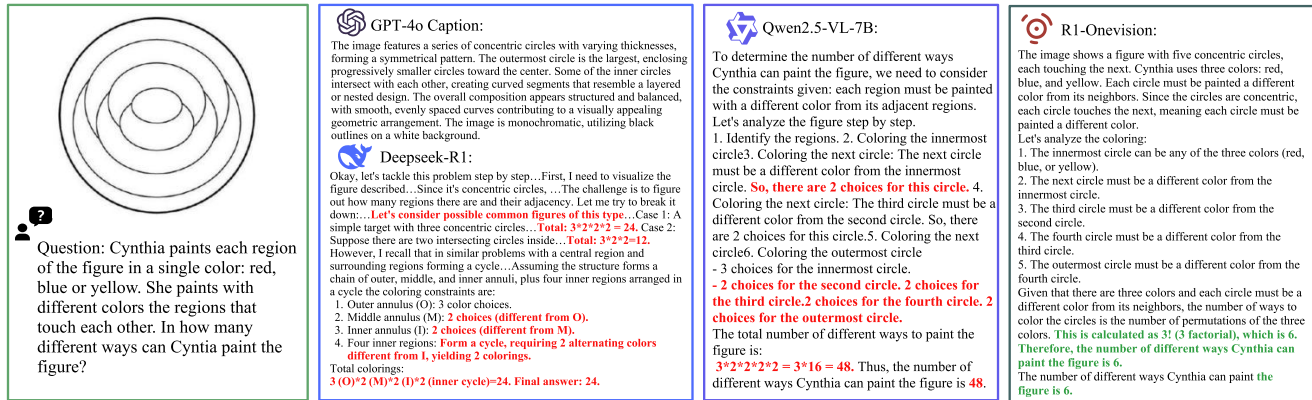


Figure 1. Comparison of baseline models and R1-Onevision. Deepseek-R1 struggles with perception errors due to GPT-4o’s incomplete image description and Qwen2.5-VL lacks the necessary reasoning ability to solve the problem. In contrast, R1-Onevision accurately interprets the image, applies structured reasoning, and arrives at the correct solution.

Abstract

Large Language Models have demonstrated remarkable reasoning capability in complex textual tasks. However, multimodal reasoning, which requires integrating visual and textual information, remains a significant challenge. Existing visual-language models often struggle to effectively analyze and reason visual content, resulting in suboptimal performance on complex reasoning tasks. Moreover, the absence of comprehensive benchmarks hinders the accurate assessment of multimodal reasoning capabilities. In this paper, we introduce R1-Onevision, a multimodal reasoning model designed to bridge the gap between visual perception and deep reasoning. To achieve this, we propose a cross-modal reasoning pipeline that transforms images into formal textural representations, enabling precise language-based reasoning. Leveraging this pipeline, we construct the R1-Onevision dataset which provides detailed, step-by-step multimodal reasoning annotations across diverse domains. We further develop the R1-Onevision model through supervised fine-tuning and reinforcement learning

*Equal contribution

to cultivate advanced reasoning and robust generalization abilities. To comprehensively evaluate multimodal reasoning performance across different grades, we introduce R1-Onevision-Bench, a benchmark aligned with human educational stages, covering exams from junior high school to university and beyond. Experimental results show that R1-Onevision achieves state-of-the-art performance, outperforming models such as GPT-4o and Qwen2.5-VL on multiple challenging multimodal reasoning benchmarks.

1. Introduction

Recent language reasoning models like Deepseek-R1 [9], chain-of-thought prompting [29], Cumulative Reasoning [40] have achieved remarkable progress in solving complex problems including coding [4, 8], mathematics [6, 11], and science [28]. However, multimodal reasoning remains a largely underexplored challenge. Unlike textual reasoning, multimodal reasoning requires the model to iteratively extract, structure, and verify information from images. Existing visual-language models often fail to organize available information and conduct in-depth reasoning processes, leading to failures in visual reasoning tasks.

Current research on visual-language models has increasingly emphasized step-by-step reasoning. Some approaches, such as LLaVA-CoT [33] and Llama-V-o1 [25], employ a predefined thinking structure to constrain the model’s reasoning process, limiting its robustness and creative potential. While such structured templates improve consistency, they often lead to shallow reasoning with limited comprehension. The others, like MAMmoTH-VL [10], rely on direct imitation of curated ground-truth answers, causing models to generate responses directly without a trial-and-error manner. Consequently, these models may fail to generalize beyond their training distributions. An example of these limitations is shown in Fig. 1. Deepseek-R1 suffers from perception errors due to incomplete image descriptions from GPT-4o [20], while Qwen2.5-VL [3], despite its strong multimodal capabilities, lacks deep reasoning ability and ultimately fails to solve the problem. These challenges highlight the core limitations of current multimodal reasoning approaches, which either impose rigid frameworks that restrict generalization or fail to provide human-like thinking behavior to accurately process visual information.

In addition, there is a lack of comprehensive benchmarks for evaluating multimodal reasoning capability. Existing benchmarks used by opencompass [7] mainly focus on mathematical problems, such as MathVision [26], MathVista [18], and WeMath [23]. While some more challenging datasets, like HumanEval-V [38], Humanity’s Last Exam [21], and ZeroBench [24], aim to assess complex diagram understanding or broader knowledge proficiency. However, these benchmarks remain specialized, covering only limited aspects of reasoning.

In this work, we address these challenges by introducing a cross-modal reasoning pipeline to construct multimodal reasoning dataset, a post-training strategy to empower reasoning capabilities, and a comprehensive multimodal reasoning benchmark. First, we propose a **cross-modal reasoning pipeline** that transforms images into visual formal representations and allows language models to process and reason over images precisely. We construct the **R1-Onevision dataset** to provide a detailed step-by-step multimodal reasoning process over diverse domains, including natural scenes, charts, mathematical expressions, and science. Second, we employ a two-stage post-training strategy to train our **R1-Onevision model** with advanced reasoning abilities. The supervised fine-tuning (SFT) stage cultivates coherent thinking patterns and output structures using our R1-Onevision dataset. The reinforcement learning (RL) stage strengthen both the model’s reasoning performance and its generalization across diverse tasks. Third, to evaluate multimodal reasoning model, we introduce **R1-Onevision-Bench**, a comprehensive benchmark explicitly designed to evaluate “grade-level” reason-

ing performance across scientific domains in the human educational system: mathematics, physics, chemistry, biology, and logical deduction. Finally, extensive experiments on several benchmarks, including MathVision [26], MathVerse [39], MathVista [18], WeMath [23] and our R1-Onevision-Bench, demonstrate the superior multimodal reasoning performance of our R1-Onevision model.

Our main contributions are summarized as follows:

- We present a cross-modal reasoning pipeline to construct **R1-Onevision Dataset** which encompasses a broad spectrum of images, questions and their reasoning process.
- We introduce **R1-Onevision**, a visual-language reasoning model designed for complex problem-solving.
- We build **R1-Onevision-Bench** to assess multi-modal reasoning performance across different educational levels and subject areas in a course-aware manner.
- Extensive experiments show the superiority of R1-Onevision compared to the baseline Qwen2.5-VL model and closed-source models like GPT-4o.

2. Related Work

Multimodal Large Language Models. MLLMs have shown significant potential in a wide range of multimodal tasks. [3, 5, 19, 27] achieve excellent visual understanding ability by integrating both visual and textual data. Recently, Multimodal Large Language Models [10, 32] demonstrates the advanced reasoning abilities when interpreting visual tasks. In addition, some studies [25, 32] introduce plan-based CoT prompting to guide models to generate intermediate information for predicting final answers. LLaVA-CoT [32] introduces a novel VLM designed to conduct visual reasoning, demonstrating exceptional performance on tasks that require structured thinking and reasoning. Based on LLaVA-CoT, LlamaV-o1 [25] introduces a multi-step curriculum learning approach, where tasks are progressively organized to facilitate incremental skill acquisition and problem-solving. CoMCTS [34] introduces the concept of collective learning into “tree search” for effective and efficient reasoning-path searching and learning. In this paper, we propose R1-Onevision, which uses supervised fine-tuning and reinforcement learning during the post-training phase to generate reasoning ability to different tasks.

Large Language Model Reasoning. The development of robust reasoning capabilities in Large Language Models (LLMs) has been a focal point of research [2, 12, 16, 22]. Some LLMs understands and solves questions by learning to create each intermediate step of the reasoning involved till the final answer. For example, Chain-of-Thought (CoT) prompting, where a complex question is decomposed into intermediate reasoning steps, have shown promise in guiding LLMs to structured solutions [30, 35]. Since certain visual tasks, such as solving Sudoku puzzles, urgently re-

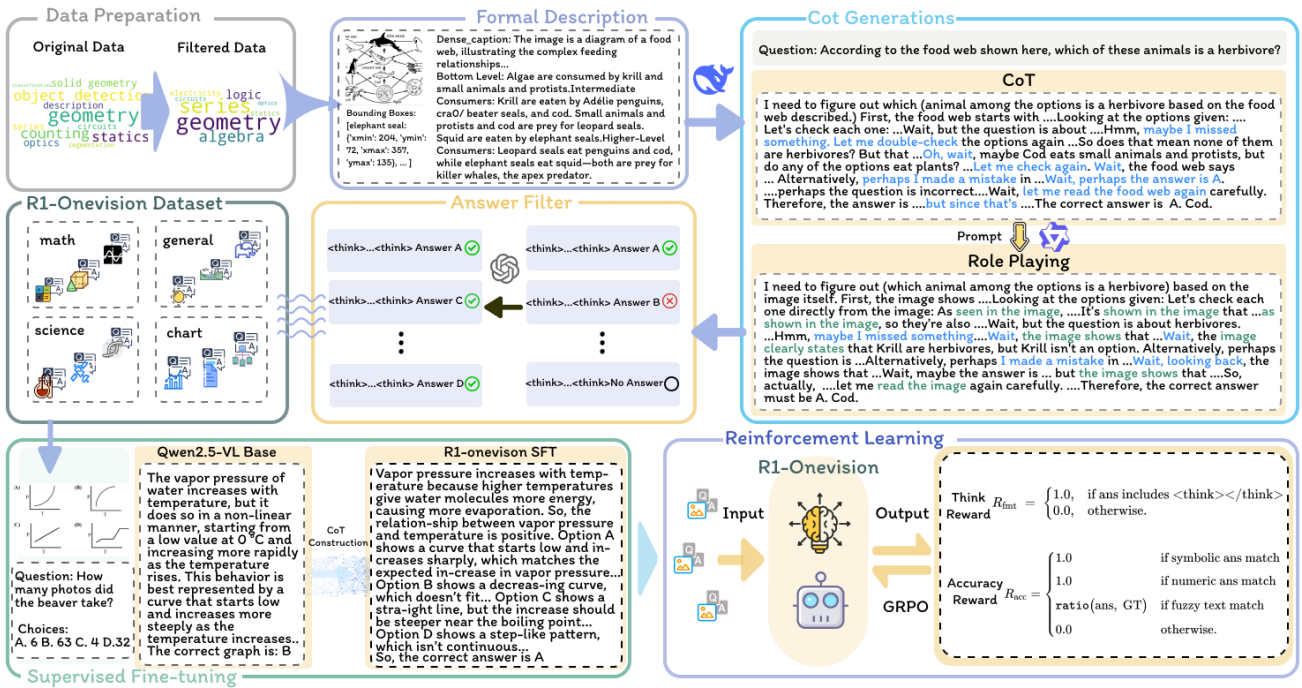


Figure 2. Overview of our R1-Onevision framework. The cross-modal reasoning pipeline begins with data preparation, integrating visual formal descriptions to enhance reasoning. We employ role-playing strategies to generate the R1-Onevision dataset with high-quality reasoning data. Post-training consists of supervised fine-Tuning to learn reasoning manner, followed by rule-based Reinforcement Learning to improve generalization across multimodal tasks.

quire multimodal large language models (MLLMs) to provide step-by-step reasoning capabilities, it is crucial to develop appropriate methods to enhance the performance of multimodal foundational models.

Visual Reasoning Benchmarks. With the advancement of model capabilities in visual reasoning, an increasing number of studies have proposed various benchmarks to evaluate the reasoning abilities of these models [13, 15, 37]. MATH-Vision (MATH-V) [26] dataset collects 3,040 high-quality mathematical problems with visual contexts sourced from real math competitions. DynaMATH [41] provides a dynamic visual math benchmark specifically designed to evaluate the mathematical reasoning robustness of VLMs. In this paper, we introduce a comprehensive benchmark designed to evaluate “grade-level” reasoning performance across scientific domains in the educational system.

3. Method

Multimodal reasoning requires a comprehensive understanding of both visual and textual modalities, yet existing models often fails to understand structured visual content and struggle with high-level reasoning. To bridge this gap, we introduce a cross-modal reasoning pipeline that transfers reasoning capabilities of language models to visual modal

through visual formal representations. Further, we employ a post-training strategy to stabilize reasoning processes and improve generalization across diverse multimodal tasks.

3.1. Cross-Modal Reasoning Pipeline

Our cross-modal reasoning pipeline is designed to bridge the gap between language reasoning models and vision models by integrating visual formal representations. Formal language is a structured system with strict syntactic and semantic constraints that eliminate ambiguity, ensuring logical consistency. With formal description of visual contents, language reasoning models are able to see and reason over image elements. We use DeepSeek R1 [9] to generate reasoning processes on LLaVA-OneVision [17] and collect these data into the R1-Onevision dataset. Figure 2 provides the process of cross-modal reasoning. Examples of the generated data are provided in the supplementary.

Data Curation and Filtering. For visual reasoning, we aggregate diverse multimodal datasets covering natural images, OCR-based text extraction, charts, mathematical expressions, and scientific reasoning problems, selecting only those that support structured reasoning. The final dataset incorporates components from the LLaVA-OneVision dataset [17], augmented with domain-specific datasets tailored for

complex inference tasks.

Image Formal Description. A key feature of our pipeline lies in its use of formal language-based annotations. To achieve this, we leveraged a combination of GPT-4o, Grounding DINO, and EasyOCR to translate visual image content into textural formal description. We outline the annotation process below and provide details of the prompt design in the supplementary.

- **Charts & Diagrams:** We prompt GPT-4o to generate structured representations, such as SPICE for circuit schematics, PlantUML or Mermaid.js for flowcharts, HTML for UI layouts, CSV/JSON for tables, and Matplotlib for annotated charts.
- **Natural Scenes:** We enhance images with fine-grained spatial description by leveraging Grounding DINO to extract bounding box annotations of key elements and GPT-4o to generate descriptive captions.
- **Text-only Images:** When dealing with images containing printed or handwritten text, we employ EasyOCR to extract text with positions and use GPT-4o to reconstruct the original document.
- **Images with Visual and Textual Content:** We integrate GPT-4o-generated captions, Grounding DINO bounding boxes, and EasyOCR-extracted text to ensure both textual and visual elements are accurately captured.
- **Mathematical Images:** For images containing mathematical content, we employ GPT-4o to propose reasoning strategies to guide the inference process.

Reasoning Process Generation. Given an image, we prompt language reasoning model with its dense captions and questions to construct cross-modal Chain-of-Thought (CoT) data. While the original Chain-of-Thought (CoT) approach offered a structured reasoning path based on textual captions, it inherently lacked the essential visual component—the ability to directly “see” and interpret the image. To address this limitation, we propose a **Role-Playing strategy** that emulates human-like visual comprehension. This method involves iteratively revisiting the image, refining its understanding, and enhancing the fidelity of the reasoning process. This process improves multimodal coherence and ensures contextually rich reasoning process.

Quality Assurance. To ensure the reliability of generated reasoning process, we employ GPT-4o to remove inaccurate, irrelevant, or inconsistent CoT steps. This step guarantees a high-quality dataset for multimodal reasoning.

R1-Onevision Dataset. Finally, as shown in the Figure 3, the R1-Onevision dataset is a carefully crafted tool designed to push the boundaries of multimodal reasoning. R1-Onevision encompasses a wide range of domains, including science, mathematics, chart data, and general real-world scenarios, totaling over 155k carefully curated samples. R1-Onevision serves as a rich resource for developing

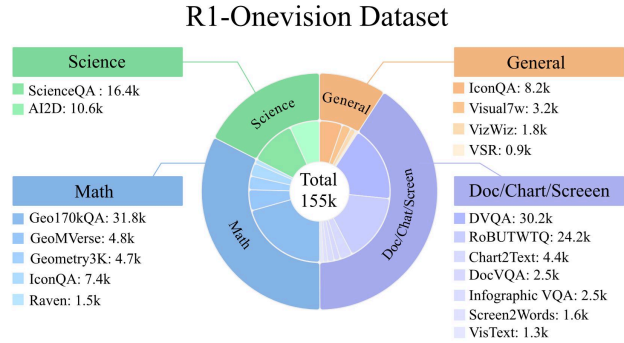


Figure 3. The data distribution of R1-Onevision dataset. R1-Onevision consists of 155k data, including Science, Math, General and Doc/Chart/Screen.

visual reasoning model.

3.2. Post-Training Strategy

To enhance multimodal reasoning capabilities, we introduce a two-stage post-training strategy consisting of Supervised Fine-Tuning (SFT) and rule-based Reinforcement Learning (RL). SFT stabilizes the model’s reasoning process and standardizes its output format, while RL further improves generalization across diverse multimodal tasks.

3.2.1. Supervised Finetuning

Leveraging the R1-Onevision dataset, we enhance the reasoning capabilities of visual language models through SFT. SFT stabilizes the model output format and cultivates a more sophisticated reasoning process in the large-scale model. This approach not only standardizes the output but also lays a solid foundation, enabling subsequent RL to achieve significant performance gains.

3.2.2. Reinforcement Learning on the SFT Model

Building upon the SFT-trained model, we employ rule-based reinforcement learning (RL) to optimize structured reasoning and ensure output validity. Specifically, we define two reward rules inspired by R1 and update the model using Group Relative Policy Optimization (GRPO). The RL stage further encourages the model to generate reliable outputs and enhances the generalizability of the model.

Rule-Based Rewards. We define two reward rules that evaluate the generated answers from two perspectives:

- **Accuracy Reward:** The accuracy reward rule evaluates the correctness of the final answer by extracting final answer via regular expressions and verifying them against the ground truth. For deterministic tasks such as math problems, the final answer must be provided in a specified format (e.g., within a box) to enable reliable rule-based verification. In cases like object detection, the reward is determined by the Intersection over Union (IoU)

score with the ground truth.

- **Format Reward:** In order to ensure the existence of the reasoning process, the format reward rule requires that the response must follow a strict format where the model’s reasoning is enclosed between `<think>` and `</think>`. A regular expression ensures the presence and correct ordering of these reasoning markers.

Group Relative Policy Optimization. We employ GRPO to achieve balanced integration of consistent policy updates and robust reward signals in a controlled manner. For each token in the generated answer, GRPO first compute the log probabilities under both the new policy ($\pi(\theta)$) and a reference policy. GRPO then calculate a ratio of these probabilities and clip it to the range $[1 - \epsilon, 1 + \epsilon]$ to prevent overly large updates. The normalized reward (serving as the advantage) is used in a PPO-style loss:

$$\mathcal{L}_{\text{clip}} = -\mathbb{E} \left[\min \left(\text{ratio}_t \cdot \text{Adv}_t, \text{clipped_ratio}_t \cdot \text{Adv}_t \right) \right].$$

Here, Adv_t denotes the advantage function, capturing how much better (or worse) a particular action is compared to a baseline policy value.

To further maintain closeness to the reference distribution, a KL divergence penalty (weighted by β) is added, yielding the overall loss:

$$\mathcal{L}_{\text{GRPO}}(\theta) = -\mathbb{E} \left[\min \left(\text{ratio}_t \cdot \text{Adv}_t, \text{clipped_ratio}_t \cdot \text{Adv}_t \right) - \beta \cdot \text{KL} \left(\pi_{\theta}(y | x), \pi_{\text{ref}}(y | x) \right) \right].$$

Compared to other methods, the GRPO clipping mechanism prevents extreme policy shifts, while the KL regularization keeps the updated policy aligned with the baseline. This combination ensures that our model integrates rule-based rewards efficiently without compromising training stability.

4. Multimodal Reasoning Benchmark

To assess the reasoning capabilities of our R1-Onevision model, we introduce a dedicated multimodal reasoning benchmark—R1-Onevision-Bench. This benchmark is designed to comprehensively evaluate the model’s performance across a wide spectrum of reasoning tasks, spanning multiple domains such as mathematics, physics, chemistry, biology, and logical deduction.

Inspired by human educational progression, R1-Onevision-Bench is structured to reflect graded levels of complexity. It includes real-world reasoning tests at the middle school, high school, and university levels, alongside a social test. This design not only mirrors the stages of cognitive development but also ensures that the evaluation covers both academic and practical reasoning skills.

Statistic	Number
Total questions	942
- Multiple-choice questions	783 (83.1%)
- Free-form questions	159 (16.9%)
- Newly collected questions	942 (100.0%)
Grades/Categories/Subcategories	4/5/38
Number of unique images	938 (99.6%)
Number of unique questions	942 (100.0%)
Number of unique answers	152 (16.1%)
Maximum question length	390
Maximum answer length	54
Average question length	127.2
Average answer length	2.1

Table 1. Key statistics of R1-Onevision-Bench.

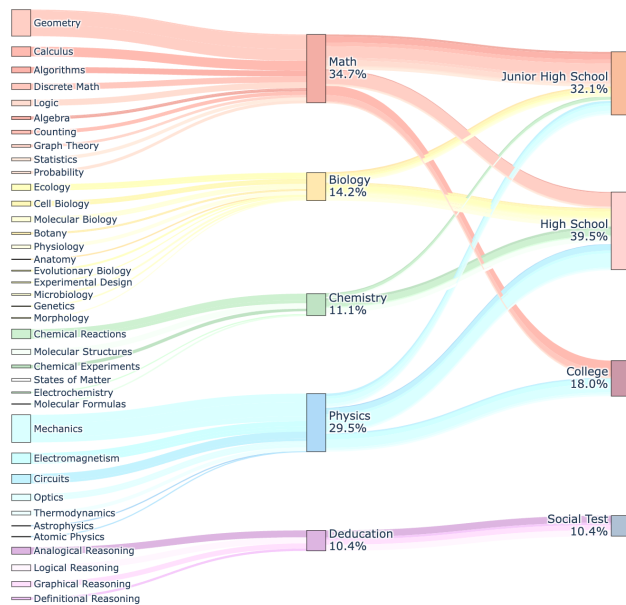


Figure 4. Overview of R1-Onevision-Bench. R1-Onevision-Bench comprises 38 subcategories organized into 5 major domains, including Math, Biology, Chemistry, Physics, Deduction. Additionally, the tasks are categorized into five levels of difficulty, ranging from ‘Junior High School’ to ‘Social Test’ challenges, ensuring a comprehensive evaluation of model capabilities across varying complexities.

By integrating diverse problem types and difficulty levels, R1-Onevision-Bench provides a rigorous framework for benchmarking multimodal reasoning. This enables us to better evaluate the grade at which multimodal language models exhibit reasoning capabilities and identify which aspects of knowledge and experience require supplementation to further enhance their performance.

Moreover, our benchmark further subdivides each cate-

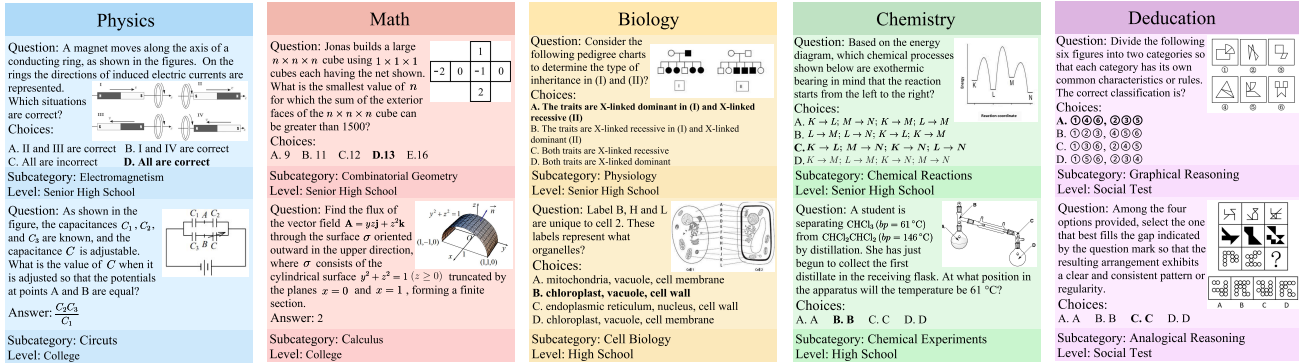


Figure 5. Samples across each category from R1-Onevision-Bench. R1-Onevision-Bench comprises multi-modal questions and answers in math, physics, chemistry, biology and deduction across multiple educational grades that require deep thinking and reasoning.

gory into specific subcategories. Figure 5 presents the detailed distribution of tasks across various categories, subcategories, and grade levels, along with examples of data from multiple domains.

5. Experiment

In this section, we first introduce the Experimental Setup of R1-Onevision in Section 5.1. Then, we present the main results in Section 5.2, demonstrating the effectiveness of R1-Onevision. Section 5.3 conduct a detailed evaluation of various models on the benchmark, including open-source and closed-source models, thoroughly assessing their performance across different grades and categories. Additionally, Section 5.3 provides an in-depth analysis of the areas where these models exhibit weaknesses, identifying specific challenges and limitations that hinder their effectiveness. Finally, Section 5.4 conducts a systematic analysis to evaluate the importance of various components during the training process.

5.1. Experimental Setup

We evaluate R1-Onevision on several multimodal reasoning benchmarks, including MathVista [18], MathVision [26], MathVerse [39] and WeMath [23]. (1) **MathVista**: a math benchmark designed to combine challenges from diverse mathematical and visual tasks. We use the Test Mini split, around 1000 samples. (2) **MathVision**: a meticulously curated collection of 3,040 high-quality mathematical problems with visual contexts sourced from real math competitions. We use the Test Mini split, consisting of 304 samples. (3) **MathVerse**: an all-around visual math benchmark designed for an equitable and in-depth evaluation of MLLMs. We apply the full dataset and also report the ‘Vision-Only’ result which unveils the great challenge by rendering the whole question within the diagram. (4) **WeMath**: a benchmark designed to explore the problem-solving principles beyond the end-to-end performance. We adopt the Test

Mini split of WeMath, around 1740 samples, we report the average accuracy as the main metric. The performance metrics of all baseline models are derived from VLMEvalKit testing results [7].

We adopt Qwen2.5-VL series as baseline models, and conduct experiments on baselines 3B and 7B to examine the effectiveness of our method. The SFT experiments are conducted with a batch size of 128, a learning rate of 1e-5, and training over 1 epochs. Then, we perform RL on the Clevr dataset [14]. We experiment with training subsets of 10k for a single epoch each. More details about the dataset construction, the training process and the benchmark can be found in the supplementary.

5.2. Main Results

Table 2 summarizes the quantitative results, showcasing that R1-Onevision consistently outperforms state-of-the-art (SoTA) multimodal methods across the majority of benchmarks. Notably, significant accuracy improvements are observed on MathVerse and MathVision, indicating that fine-grained visual-textual alignment and coherent chain-of-thought reasoning play a critical role in enhancing performance. These results validate the effectiveness of our proposed approach in addressing the diverse challenges of multimodal reasoning tasks. Additionally, R1-Onevision achieves 29.9% accuracy in MathVision, which is comparable to the closed-source model GPT-4o. In MathVerse and MathVista, R1-Onevision surpasses the GPT-4o 5.2% (MathVerse ALL), 5.5% (MathVerse Vision Only) and 4.1% (MathVista), further demonstrating its competitiveness in improving reasoning ability.

5.3. Benchmark Analysis

We evaluate the performance of two sets of models in the R1-Onevision benchmark, which categorize into four levels of difficulty (ranging from ‘Junior High School’ to ‘Social Test’) and five distinct academic disciplines (Math,

Model	MathVision	MathVerse		MathVista	WeMath
		ALL	Vision Only		
<i>Base Model</i>					
Qwen2.5-VL-7B [3]	25.4	43.6	38.2	63.7	61.0
<i>Our Models</i>					
R1-Onevision-7B	29.9	46.4	40.0	64.1	61.8
<i>Other Models</i>					
GPT-4o [20]	30.6	41.2	34.5	60.0	69.0
InternVL2.5-8B [5]	17.1	35.6	22.8	64.5	53.8
Qwen2-VL-7B [27]	21.7	30.2	25.4	61.6	50.5
LLaVA-CoT-11B [33]	-	-	22.6	52.5	-

Table 2. Experimental results on mathematical reasoning benchmarks. Except for LLaVA-CoT-11B, all reported results are based on our reproduced experiments. The highest accuracy is marked in blue.

Model	Avg	Grade				Category				
		Junior High School	High School	College	Social Test	Math	Physics	Chemistry	Biology	Deduction
<i>Closed-source</i>										
GPT-4o	49.6	51.3	56.2	45.3	26.5	41.3	52.5	71.4	63.4	26.5
Gemini-2.0-Flash	59.1	56.0	65.9	61.2	39.8	52.3	64.4	74.3	67.2	39.8
Claude-3.5	52.1	56.0	55.9	49.4	30.6	46.5	54.3	66.7	65.7	30.6
<i>Open-source</i>										
MiniCPM-o-2.6 [36]	30.4	33.4	31.7	21.2	31.6	24.2	31.7	30.5	41.8	31.6
InternVL2.5-8B [5]	29.5	33.1	30.6	21.8	27.6	26.3	24.8	32.4	46.3	27.6
InternVL2.5-8B-MPO [5]	32.5	37.4	33.6	24.7	26.5	28.7	29.9	41.0	44.8	26.5
Qwen2-VL-7B [27]	30.0	35.4	28.5	25.9	26.5	26.3	28.1	30.5	45.5	26.5
Qwen2.5-VL-7B [3]	32.1	33.8	37.1	25.3	19.4	31.5	27.3	39.0	47.0	19.4
DeepSeek-VL2 [31]	29.8	34.4	30.9	18.8	30.6	23.5	28.4	29.5	47.8	30.6
R1-Onevision-7B	36.2	40.1	39.5	27.6	26.5	33.0	30.2	49.5	53.0	26.5
Qwen2.5-VL-72B [3]	52.0	54.3	56.7	54.1	23.5	48.9	55.8	63.8	63.4	23.5

Table 3. Evaluation results of closed-source and open-source multimodal models on R1-Onevision benchmark. We divide the benchmark into four grades (‘Junior High School’, ‘High School’, ‘College’, ‘Social Test’) and five categories (‘Math’, ‘Physics’, ‘Chemistry’, ‘Biology’, ‘Deduction’). The highest accuracy for closed-source and open-source LMMs are marked in blue and green, respectively.

Physics, Chemistry, Biology, Deduction). The first group consisted of SOTA closed-source VLMs, such as GPT-4o, Gemini-2.0-Flash and Claude-3.5. The second group comprised SOTA open-source VLMs, including MiniCPM-o-2.6, InternVL2.5-8B, InternVL2.5-8B-MPO, Qwen2-VL-7B, Qwen2.5-VL-7B, Qwen2.5-VL-72B, DeepSeek-VL2 and R1-Onevision. We deploy VLMEvalkit package to infer in various models. Additionally, we evaluate the impact of model parameters on benchmark performance by testing the Qwen2.5-VL series, specifically comparing the 7B and 72B models. This analysis provides insights into how scaling model parameters influences performance across the benchmark, offering valuable guidance for future model development and optimization. As for scoring in R1-Onevision benchmark, following MathVision and MathVerse, we use GPT-4o-mini to extract the answer and score. The prompt of extract and score process is shown in the supplementary.

Overall Results on Average Accuracy. Table 3 illustrates the average performance of a variety of closed-source and open-source models. Closed-source models, such as GPT-4o, Gemini-2.0-Flash and Claude-3.5 have demonstrated excellent performance on the leaderboard, with their average scores surpassing 50% those of other models. Notably, Gemini-2.0-Flash demonstrates robust performance across questions of varying difficulty levels, ranging from Junior High school to College-level tasks. It also excels across multiple categories, achieving scores above 50% in math, physics, chemistry and biology. Furthermore, Gemini-2.0-Flash surpasses the closed-source model GPT-4o about 10% average accuracy, demonstrating its effectiveness in reasoning ability. However, both closed-source and open-source models exhibit a stronger proficiency in tackling questions designed for middle and high school students, while their performance tends to decline on university-level and professional certification exams. Across various academic disci-

plines, all models struggle with **Deduction** questions, with none of the models exceeding 40% accuracy. Finally, while open-source models typically underperform compared to closed-source counterparts, recent advancements in models like Qwen2.5-VL-72B has significantly narrowed the gap, with Qwen2.5-VL-72B achieves 52% average accuracy. Qwen2.5-VL-72B is on par with close-source Claude-3.5, ranking just behind Gemini-2.0-Flash. As for the 4-10B models, notably, R1-Onevision, developed based on Qwen2.5-VL, has delivered outstanding results, ranking just behind the top closed-source models.

5.4. Ablation Study

5.4.1. Analysis of Training Strategy

To evaluate the effectiveness of our training data, we compare the model’s performance under two distinct training strategies: (1) applying Supervised Fine-Tuning (SFT) on our dataset, and (2) further optimizing the SFT-trained model with Reinforcement Learning (RL). As illustrated in Table 4, the application of SFT on our dataset significantly enhances the model’s performance on both the MathVision and MathVerse (Vision Only) benchmarks. Notably, the model achieves comparable results on the MathVision benchmark, demonstrating its ability to construct systematic thinking habits through our dataset. These findings underscore the value of our dataset in improving models’ reasoning capabilities, particularly in tasks requiring structured and logical problem-solving. Furthermore, as shown in Table 5, the subsequent application of RL after SFT yields additional performance gains. This step pushes the model toward deeper and more deductive thinking, enabling it to tackle more complex and nuanced problems. The incremental improvements observed highlight the complementary nature of SFT and RL: while SFT establishes a robust foundation by aligning the model with high-quality reasoning patterns, RL refines and amplifies these capabilities by encouraging more advanced cognitive processes. This study demonstrates that our training data plays a pivotal role in enhancing model performance, and the combination of SFT and RL provides a powerful and effective strategy for maximizing reasoning and thinking performance. These results validate the quality and utility of our reasoning dataset.

5.4.2. Ablation Study on Model Parameters Variants

To demonstrate the effectiveness of our approach across models of different parameter sizes, we conducted a series of ablation experiments using Qwen2.5-VL-3B as a smaller base model. Specifically, we applied both Supervised Fine-Tuning (SFT) and Reinforcement Learning (RL) to the Qwen2.5VL-3B model and evaluated its performance. The experimental results, as summarized in Table 6, reveal significant improvements in reasoning and task performance comparing with the base Qwen2.5-VL-3B. R1-Onevision-

Model	MathVision	MathVerse	MathVerse (Vision Only)
Qwen2.5-VL-7B	25.4	43.6	38.2
SFT	26.3	43.4	39.7
SFT+RL	29.9	46.4	40.0

Table 4. Ablation study on training strategies. The best results are marked in blue .

Benchmark	SFT+RL	RL
MathVision	29.9	28.0

Table 5. Comparison of MathVision performance between SFT+RL and RL. The best results are marked in blue .

Model	MathVision	MathVerse	MathVerse (Vision Only)
Qwen2.5-VL-3B	21.7	34.7	31.2
R1-Onevision-3B	23.7	38.6	35.5

Table 6. Evaluation of our method using Qwen2.5-VL-3B base model on MathVision, MathVerse and MathVerse (Vision Only). The best results are marked in blue .

3B achieves 23.6% accuracy in MathVision, 38.6% in MathVerse (ALL). This performance significantly surpasses that of our base model, demonstrating a remarkable improvement in reasoning capabilities. These findings highlight the scalability and adaptability of our method, showing that it remains effective across different model sizes.

6. Conclusion

In this paper, we introduce a comprehensive framework for multimodal reasoning, built upon a cross-modal formalization approach that unifies data construction, model training, and evaluation. Our framework is designed to address the inherent challenges of integrating visual and textual modalities, enabling models to reason effectively across these domains. The cross-modal reasoning pipeline at the core of this framework bridges the gap between vision and language by leveraging fine-grained alignment mechanisms and structured reasoning pathways. This framework has led to the creation of the R1-Onevision dataset, a rich resource featuring detailed step-by-step reasoning annotations designed to enhance model training and evaluation. The R1-Onevision model, trained using this framework, demonstrates strong multimodal reasoning capabilities and exhibits robust generalization across a diverse range of tasks, from visual question answering to complex problem-solving scenarios. To further support the evaluation of multimodal reasoning, we introduce R1-Onevision-Bench, a comprehensive benchmark that rigorously assesses model performance across various dimensions of reasoning. Our extensive experiments

validate the effectiveness of our approach, showing significant improvements over state-of-the-art open-source models.

References

- [1] Josh Achiam, Steven Adler, Sandhini Agarwal, Lama Ahmad, Ilge Akkaya, Florencia Leoni Aleman, Diogo Almeida, Janko Altenschmidt, Sam Altman, Shyamal Anadkat, et al. Gpt-4 technical report. *arXiv preprint arXiv:2303.08774*, 2023. 12
- [2] Janice Ahn, Rishu Verma, Renze Lou, Di Liu, Rui Zhang, and Wenpeng Yin. Large language models for mathematical reasoning: Progresses and challenges. *arXiv preprint arXiv:2402.00157*, 2024. 2
- [3] Shuai Bai, Keqin Chen, Xuejing Liu, Jialin Wang, Wenbin Ge, Sibong Song, Kai Dang, Peng Wang, Shijie Wang, Jun Tang, et al. Qwen2. 5-vl technical report. *arXiv preprint arXiv:2502.13923*, 2025. 2, 7
- [4] Mark Chen, Jerry Tworek, Heewoo Jun, Qiming Yuan, Henrique Ponde De Oliveira Pinto, Jared Kaplan, Harri Edwards, Yuri Burda, Nicholas Joseph, Greg Brockman, et al. Evaluating large language models trained on code. *arXiv preprint arXiv:2107.03374*, 2021. 1
- [5] Zhe Chen, Weiyun Wang, Yue Cao, Yangzhou Liu, Zhangwei Gao, Erfei Cui, Jinguo Zhu, Shenglong Ye, Hao Tian, Zhaoyang Liu, et al. Expanding performance boundaries of open-source multimodal models with model, data, and test-time scaling. *arXiv preprint arXiv:2412.05271*, 2024. 2, 7
- [6] Karl Cobbe, Vineet Kosaraju, Mohammad Bavarian, Mark Chen, Heewoo Jun, Lukasz Kaiser, Matthias Plappert, Jerry Tworek, Jacob Hilton, Reiichiro Nakano, et al. Training verifiers to solve math word problems. *arXiv preprint arXiv:2110.14168*, 2021. 1
- [7] OpenCompass Contributors. Opencompass: A universal evaluation platform for foundation models, 2023. 2, 6
- [8] Alex Gu, Baptiste Rozière, Hugh Leather, Armando Solar-Lezama, Gabriel Synnaeve, and Sida I Wang. Cruxeval: A benchmark for code reasoning, understanding and execution. In *International Conference on Machine Learning*, 2024. 1
- [9] Daya Guo, Dejian Yang, Haowei Zhang, Junxiao Song, Ruoyu Zhang, Runxin Xu, Qihao Zhu, Shirong Ma, Peiyi Wang, Xiao Bi, et al. Deepseek-r1: Incentivizing reasoning capability in llms via reinforcement learning. *arXiv preprint arXiv:2501.12948*, 2025. 1, 3
- [10] Jarvis Guo, Tuney Zheng, Yuelin Bai, Bo Li, Yubo Wang, King Zhu, Yizhi Li, Graham Neubig, Wenhui Chen, and Xiang Yue. Mammoth-vl: Eliciting multimodal reasoning with instruction tuning at scale. *arXiv preprint arXiv:2412.05237*, 2024. 2
- [11] Dan Hendrycks, Collin Burns, Saurav Kadavath, Akul Arora, Steven Basart, Eric Tang, Dawn Song, and Jacob Steinhardt. Measuring mathematical problem solving with the MATH dataset. In *Proceedings of the Neural Information Processing Systems Track on Datasets and Benchmarks*, 2024. 1
- [12] Jie Huang and Kevin Chen-Chuan Chang. Towards reasoning in large language models: A survey. *arXiv preprint arXiv:2212.10403*, 2022. 2
- [13] Drew A Hudson and Christopher D Manning. Gqa: A new dataset for real-world visual reasoning and compositional question answering. In *Proceedings of the IEEE/CVF conference on computer vision and pattern recognition*, pages 6700–6709, 2019. 3
- [14] Justin Johnson, Bharath Hariharan, Laurens van der Maaten, Li Fei-Fei, C. Lawrence Zitnick, and Ross Girshick. Clevr: A diagnostic dataset for compositional language and elementary visual reasoning, 2016. 6
- [15] Samira Ebrahimi Kahou, Vincent Michalski, Adam Atkinson, Ákos Kádár, Adam Trischler, and Yoshua Bengio. Figureqa: An annotated figure dataset for visual reasoning. In *International Conference on Learning Representations Workshop Track*, 2018. 3
- [16] Takeshi Kojima, Shixiang Shane Gu, Machel Reid, Yutaka Matsuo, and Yusuke Iwasawa. Large language models are zero-shot reasoners. *Advances in neural information processing systems*, 35:22199–22213, 2022. 2
- [17] Bo Li, Yuanhan Zhang, Dong Guo, Renrui Zhang, Feng Li, Hao Zhang, Kaichen Zhang, Peiyuan Zhang, Yanwei Li, Ziwei Liu, and Chunyuan Li. LLaVA-onevision: Easy visual task transfer. *Transactions on Machine Learning Research*, 2025. 3
- [18] Pan Lu, Hritik Bansal, Tony Xia, Jiacheng Liu, Chunyuan Li, Hannaneh Hajishirzi, Hao Cheng, Kai-Wei Chang, Michel Galley, and Jianfeng Gao. Mathvista: Evaluating mathematical reasoning of foundation models in visual contexts. In *The Twelfth International Conference on Learning Representations*, 2024. 2, 6, 12
- [19] AI Meta. Llama 3.2: Revolutionizing edge ai and vision with open, customizable models. *Meta AI Blog*. Retrieved December, 20:2024, 2024. 2
- [20] OpenAI. Gpt-4o system card, 2024. 2, 7
- [21] Long Phan, Alice Gatti, Ziwen Han, Nathaniel Li, Josephina Hu, Hugh Zhang, Sean Shi, Michael Choi, Anish Agrawal, Arnav Chopra, et al. Humanity’s last exam. *arXiv preprint arXiv:2501.14249*, 2025. 2
- [22] Aske Plaat, Annie Wong, Suzan Verberne, Joost Broekens, Niki van Stein, and Thomas Back. Reasoning with large language models, a survey. *arXiv preprint arXiv:2407.11511*, 2024. 2
- [23] Runqi Qiao, Qiuna Tan, Guanting Dong, Minhui Wu, Chong Sun, Xiaoshuai Song, Zhuoma Gongque, Shanglin Lei, Zhe Wei, Miaoxuan Zhang, et al. We-math: Does your large multimodal model achieve human-like mathematical reasoning? *arXiv preprint arXiv:2407.01284*, 2024. 2, 6
- [24] Jonathan Roberts, Mohammad Reza Taesiri, Ansh Sharma, Akash Gupta, Samuel Roberts, Ioana Croitoru, Simion-Vlad Bogolin, Jialu Tang, Florian Langer, Vyas Raina, et al. Zerobench: An impossible visual benchmark for contemporary large multimodal models. *arXiv preprint arXiv:2502.09696*, 2025. 2
- [25] Omkar Thawakar, Dinura Dissanayake, Ketan More, Ritesh Thawkar, Ahmed Heakl, Noor Ahsan, Yuhao Li, Mohammed

- Zumri, Jean Lahoud, Rao Muhammad Anwer, et al. Llamav-01: Rethinking step-by-step visual reasoning in llms. *arXiv preprint arXiv:2501.06186*, 2025. [2](#)
- [26] Ke Wang, Junting Pan, Weikang Shi, Zimu Lu, Houxing Ren, Aojun Zhou, Mingjie Zhan, and Hongsheng Li. Measuring multimodal mathematical reasoning with math-vision dataset. *Advances in Neural Information Processing Systems*, 37:95095–95169, 2025. [2](#), [3](#), [6](#), [12](#)
- [27] Peng Wang, Shuai Bai, Sinan Tan, Shijie Wang, Zhihao Fan, Jinze Bai, Keqin Chen, Xuejing Liu, Jialin Wang, Wenbin Ge, et al. Qwen2-vl: Enhancing vision-language model’s perception of the world at any resolution. *arXiv preprint arXiv:2409.12191*, 2024. [2](#), [7](#)
- [28] Yubo Wang, Xueguang Ma, Ge Zhang, Yuansheng Ni, Abhramil Chandra, Shiguang Guo, Weiming Ren, Aaran Arulraj, Xuan He, Ziyang Jiang, et al. Mmlu-pro: A more robust and challenging multi-task language understanding benchmark. In *Advances in Neural Information Processing Systems*, 2024. [1](#)
- [29] Jason Wei, Xuezhi Wang, Dale Schuurmans, Maarten Bosma, Fei Xia, Ed Chi, Quoc V Le, Denny Zhou, et al. Chain-of-thought prompting elicits reasoning in large language models. *Advances in neural information processing systems*, 35:24824–24837, 2022. [1](#)
- [30] Yixuan Weng, Minjun Zhu, Fei Xia, Bin Li, Shizhu He, Shengping Liu, Bin Sun, Kang Liu, and Jun Zhao. Large language models are better reasoners with self-verification. *arXiv preprint arXiv:2212.09561*, 2022. [2](#)
- [31] Zhiyu Wu, Xiaokang Chen, Zizheng Pan, Xingchao Liu, Wen Liu, Damai Dai, Huazuo Gao, Yiyang Ma, Chengyue Wu, Bingxuan Wang, Zhenda Xie, Yu Wu, Kai Hu, Jiawei Wang, Yaofeng Sun, Yukun Li, Yishi Piao, Kang Guan, Aixin Liu, Xin Xie, Yuxiang You, Kai Dong, Xingkai Yu, Haowei Zhang, Liang Zhao, Yisong Wang, and Chong Ruan. Deepseek-vl2: Mixture-of-experts vision-language models for advanced multimodal understanding, 2024. [7](#)
- [32] Guowei Xu, Peng Jin, Li Hao, Yibing Song, Lichao Sun, and Li Yuan. Llava-o1: Let vision language models reason step-by-step. *arXiv preprint arXiv:2411.10440*, 2024. [2](#)
- [33] Guowei Xu, Peng Jin, Hao Li, Yibing Song, Lichao Sun, and Li Yuan. Llava-cot: Let vision language models reason step-by-step, 2025. [2](#), [7](#)
- [34] Huanjin Yao, Jiaying Huang, Wenhao Wu, Jingyi Zhang, Yibo Wang, Shunyu Liu, Yingjie Wang, Yuxin Song, Haocheng Feng, Li Shen, et al. Mulberry: Empowering mllm with o1-like reasoning and reflection via collective monte carlo tree search. *arXiv preprint arXiv:2412.18319*, 2024. [2](#)
- [35] Shunyu Yao, Dian Yu, Jeffrey Zhao, Izhak Shafran, Tom Griffiths, Yuan Cao, and Karthik Narasimhan. Tree of thoughts: Deliberate problem solving with large language models. *Advances in neural information processing systems*, 36:11809–11822, 2023. [2](#)
- [36] Yuan Yao, Tianyu Yu, Ao Zhang, Chongyi Wang, Junbo Cui, Hongji Zhu, Tianchi Cai, Haoyu Li, Weilin Zhao, Zhihui He, et al. Minicpm-v: A gpt-4v level mllm on your phone. *arXiv preprint arXiv:2408.01800*, 2024. [7](#)
- [37] Chi Zhang, Feng Gao, Baoxiong Jia, Yixin Zhu, and Song-Chun Zhu. Raven: A dataset for relational and analogical visual reasoning. In *Proceedings of the IEEE/CVF conference on computer vision and pattern recognition*, pages 5317–5327, 2019. [3](#)
- [38] Fengji Zhang, Linqun Wu, Huiyu Bai, Guancheng Lin, Xiao Li, Xiao Yu, Yue Wang, Bei Chen, and Jacky Keung. Humaneval-v: Evaluating visual understanding and reasoning abilities of large multimodal models through coding tasks. *arXiv preprint arXiv:2410.12381*, 2024. [2](#)
- [39] Renrui Zhang, Dongzhi Jiang, Yichi Zhang, Haokun Lin, Ziyu Guo, Pengshuo Qiu, Aojun Zhou, Pan Lu, Kai-Wei Chang, Yu Qiao, Peng Gao, and Hongsheng Li. Mathverse: Does your multi-modal llm truly see the diagrams in visual math problems? In *European Conference on Computer Vision*, page 169–186, 2024. [2](#), [6](#)
- [40] Yifan Zhang, Jingqin Yang, Yang Yuan, and Andrew Chi-Chih Yao. Cumulative reasoning with large language models. *arXiv preprint arXiv:2308.04371*, 2023. [1](#)
- [41] Chengke Zou, Xingang Guo, Rui Yang, Junyu Zhang, Bin Hu, and Huan Zhang. Dynamath: A dynamic visual benchmark for evaluating mathematical reasoning robustness of vision language models. *arXiv preprint arXiv:2411.00836*, 2024. [3](#)

Roadmap of Appendix

The structure of the appendix is delineated as follows: Descriptions of the relevant experimental details are provided in the Section A. Subsequently, Section B encompasses a presentation of supplementary visualization results.

A. More Implementation Details

A.1. Data Details

Our cross-modal reasoning pipeline consists of: Data Curation and Filtering, Image Formal Description, Reasoning Process Generation and Quality Assurance. We adapt the following prompt in Reasoning Process Generation.

Answer the question and provide your reasoning process, including the following:

1. Simulate image reasoning: Treat the image caption as an image. Simulate reasoning by imagining you are looking at the image, and act as if you can see it. However, avoid visualization as a step in the reasoning process.
2. Direct visual language: Frame observations as if you are directly viewing the image (e.g., “The image shows...”). Avoid reasoning through image caption or description.
3. Forbidden phrases: Avoid phrases like “based on the caption”, “based on the description”, “visualizing the image”.

Question: {*question*}

Image Content: {*caption*}.

Then, we introduce “role play” to bridge the gap in real image understanding and then filter the data. The prompts are as follows:

Revise the provided Chain of Thought (CoT) to follow these guidelines:

1. Style Shift: Convert all references to image description-based reasoning into direct image-based reasoning. For example: Replace phrases like “based on the description” “based on the caption” with “the image shows” or “as seen in the image”.
2. Remove image visualization step: If the CoT contains an inference step for image visualization, remove it and rewrite the CoT to reflect reasoning directly on the image itself, rather than reasoning after visualization from the image description.

Apply these changes rigorously to ensure that the final CoT reflects direct image interpretation, uninfluenced by description, caption, image visualization.

CoT: {*cot*}

Give your assistant’s response. This response is the reasoning steps for the assistant to solve the problem. Please follow the following rules to evaluate whether the assistant’s response is valid.

Rules for judging as valid:

1. The assistant’s response has correct reasoning steps.
2. The assistant’s response has the final reasoning answer, and the final reasoning answer is consistent with the meaning of the standard answer.
3. The assistant’s response is based on the reasoning process of the image, not the image description or caption.
4. There are no steps in the assistant’s response that are irrelevant to the reasoning, and each reasoning step is closely related.

Standard answer: {*gt*}

Assistant’s response: {*augmented answer*}

Output:

A.2. Model Details

For model training, we utilized the llama-factory and adopted a full fine-tuning strategy to optimize the model’s performance. Following this, we further refined the model through Reinforcement Learning (RL). During the inference phase, the RL-tuned model was evaluated using a fixed prompt to ensure consistent and reliable results. The prompt is defined as: “**First output the thinking process in <think> </think> tags and then output the final answer in <answer> </answer> tags.**”.

A.3. Evaluation Details

To evaluate the reasoning capabilities of the models, we adopted a unified evaluation framework for both public benchmarks and our benchmark R1-Onevision bench. Following [18, 26], we utilized GPT-4o-mini [1] to assess model performance. For extracting answers from Chain-of-Thought (CoT) responses, we employed the prompt **“Below is a thought process and an answer that includes the final choices. Please extract only the final choices (A, B, C, D, etc.) from the text and do not return any other words. If the final choice is not explicitly stated in the text, output NONE. No reasoning is required; just extract the answer.”** for multiple choice questions and **“The following is a thought process and a free-form answer. Please extract the numerical value or text of the final answer, excluding any explanation. If the final answer cannot be extracted from the given text, output NONE. No reasoning is required; just extract the answer.”** for free form questions. Then we score the extracted answer with the groundtruth using **“Compare ‘final answer’ with ‘groundtruth’. If final answer matches ‘groundtruth’, output YES; otherwise, output NO. Do not return any extra words. For numerical answers with units, if ‘final answer’ contains the unit but its numeric value matches ‘groundtruth’, consider it a match.”**

B. Visualization

B.1. Image Formal Description

In this section, we demonstrate some examples of image formal description.

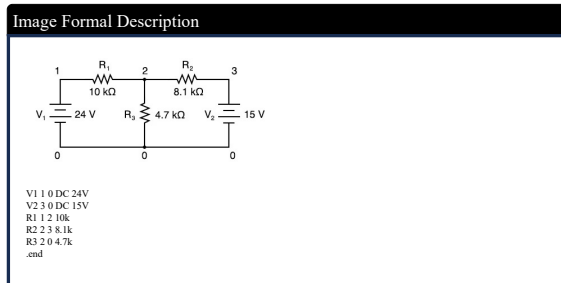


Figure 6. Formal Description of Circuits.

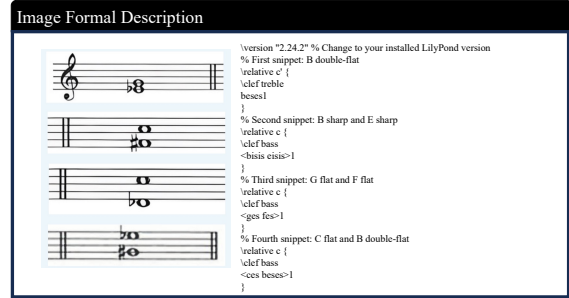


Figure 7. Formal Description of Music Sheet.

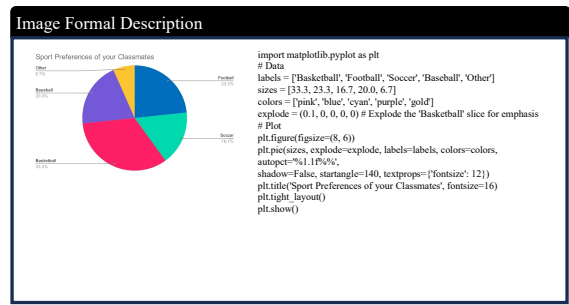


Figure 8. Formal Description of Table.



Figure 9. Formal Description of Natural Scene.

Image Formal Description

OCR Result:
 FREE OFFER
 FULL COLOR RECIPE SET. A "Good Wishes" offer for you from G W Sugar. Mail coupon today!
 Mrs. McVinn ALB Right
 (NAME PLEASE PRINT)
 Box 147
 (ADDRESS)
 BE RELEN WLS S 54943
 (City) (STATE) (Zip CODE)
 Mail to: Great Western Sugar Company
 Sales Department Room 514
 Box 5308 Denver, Colorado 80217
 Souce-nlpp5 HWV dustrydctim5: idocs DcU

Figure 10. Formal Description of print, handwriting.

Image Formal Description

Problem Description and Solution
 The image shows a geometric configuration involving triangle ABC, where line segment AB is perpendicular to segment BC. Angles within and around this configuration are labeled with numbers and measurements.
 The triangle consists of angles labeled 1, 2, and 3 at vertices A and B, and point C extends beyond these angles.
 Angle 1 measures 36°, and angle 3 is adjacent to AB and BC, with a given measure of 104°. With AB being perpendicular to BC, angle 5, which is an exterior angle at point B and forms a right angle with the horizontal, measures 90° due to perpendicularity.
 Angles 4, 6, 7, and 8 lie along line BC or are supplementary to angles at B. Angle 4 must complement angle 5 to form a straight line with angle 3, as they are on the same line.
 Therefore, angle 4 is calculated as 180° - angle 3 - angle 5 = 180° - 104° - 36° = 40°. The measure of angle 4 is thus 40°, making the correct choice (C).

Figure 11. Formal Description of Math.

Image Formal Description

Description:
 The image contains the following objects and categories: A person dressed in a Spider-Man costume standing on a stage. A table or small desk with papers on it. A microphone or other audio equipment on the stage. A projection screen displaying text. An audience seated in rows. A wooden podium on the side of the stage. A crest or emblem displayed above the screen. A classroom or hall setting with walls and flooring visible.
 OCR Result:
 Reddit should add an undo button so if you accidentally scroll to the top you can go back to where you were

Figure 12. Formal Description of MEME.

B.2. Model Reasoning Capabilities and Qualitative Examples

In this section, we present some practical examples of our R1-Onevision.

Problem

A beaver is photographing butterflies, but after each photo is taken, half the butterflies fly away.

The first photo has 64 butterflies in it and the last photo has 2 butterflies in it.

Question: How many photos did the beaver take?
 Choices:
 A. 6 B. 63 C. 4 D. 32

Response

Okay, so I'm trying to figure out how many photos the beaver took. Let me start by understanding the problem. The beaver is taking photos of butterflies, and after each photo, half the butterflies fly away. The first photo has 64 butterflies, and the last one has 2. I need to find out how many photos were taken in total.

Hmm, let's break it down. If after each photo, half the butterflies fly away, that means each time the number of butterflies is halved. So, starting with 64 butterflies, each subsequent photo would have half as many butterflies as the previous one.

Let me list out the number of butterflies in each photo:

1. First photo: 64 butterflies
2. Second photo: $64 / 2 = 32$ butterflies
3. Third photo: $32 / 2 = 16$ butterflies
4. Fourth photo: $16 / 2 = 8$ butterflies
5. Fifth photo: $8 / 2 = 4$ butterflies
6. Sixth photo: $4 / 2 = 2$ butterflies

So, the beaver took six photos in total. Each time, the number of butterflies is halved, and after six photos, only 2 butterflies remain.

Therefore, the beaver took 6 photos.

The beaver took 6 photos.

Answer: A

Figure 13. The model displays an adeptness in processing math.

Problem

In the figure shown, the mass $m=6.0$ kg and the mass $M=14.0$ kg are stationary. The mass m rests on the floor. Which one of the following choices represents the tension in the string connecting the masses?

A. 40 N
 B. 60 N
 C. 80 N
 D. 140 N
 E. 200 N

Response

The image shows a pulley system with two masses, $m=6.0$ kg and $M=14.0$ kg. The smaller mass m is hanging from the pulley, and the larger mass M is on the floor. The tension in the string connecting them is what we need to find.

Since the system is stationary, the forces acting on each mass must balance. The tension in the string is the same on both sides of the pulley. For mass m , the tension (T) is equal to its weight, which is $m \cdot g$. For mass M , the tension is also T , but it is acting upwards to counteract the gravitational force.

The gravitational force on mass m is $6.0 \text{ kg} \cdot 9.8 \text{ m/s}^2 = 58.8 \text{ N}$. The gravitational force on mass M is $14.0 \text{ kg} \cdot 9.8 \text{ m/s}^2 = 137.2 \text{ N}$. Since the system is stationary, the tension in the string must be equal to the gravitational force on the smaller mass, which is 58.8 N. However, the options provided are 40 N, 60 N, 80 N, 140 N, and 200 N. The closest value to 58.8 N among the options is 60 N.

Therefore, the tension in the string is 60 N.

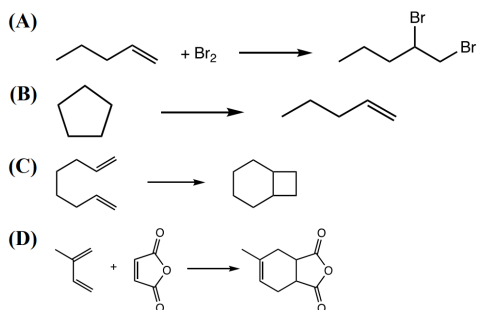
Answer: B

The tension in the string is determined by the gravitational force on the smaller mass, which is 60 N.

Answer: B

Figure 14. The model displays an adeptness in processing physics.

Problem



Question: Which reaction has $\Delta S_{\text{rxn}}^{\circ} > 0$? All reactants and products are liquids.

Choices:

- A. A
- B. B
- C. C
- D. D

Response

Okay, so I need to figure out which reaction among the four options has a positive standard entropy change, denoted as $\Delta S^{\circ}_{\text{rxn}} > 0$. The hint says all reactants and products are liquids, which is important because the state of matter affects the entropy change.

Looking at each option:

Option A: The image shows a reaction where a pentene is brominated. The reactant is a liquid, and the product is a liquid. Bromination typically involves adding bromine atoms, which might form a new compound. Since both are liquids, the change in state isn't a factor here. The reaction is likely exothermic, but without knowing the exact products, it's hard to say if ΔS° is positive or negative.

Option B: The image shows a cyclopentene being converted into a hexene. Cyclopentene is a liquid, and hexene is also a liquid. The reaction involves breaking a ring and forming a double bond. This usually increases the number of degrees of freedom, leading to a higher entropy. So ΔS° should be positive here.

Option C: The image shows a reaction where a diene forms a cyclobutane. Both reactants and products are liquids. Diene to cyclobutane is a ring closure, which reduces the number of degrees of freedom. This would decrease the entropy, making ΔS° negative.

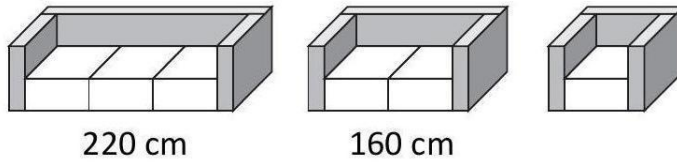
Option D: The image shows a Diels-Alder reaction between a diene and a dienophile. Both are liquids. The products are a cyclohexene and a ketone. The formation of a six-membered ring might increase the entropy, but the overall change depends on the specific reactants and products. However, since both are liquids, the state change isn't a factor.

Considering the state of matter, all reactions involve liquids, so the main factor is the type of reaction. Option B involves breaking a ring and forming a double bond, which increases the number of degrees of freedom, leading to a positive ΔS° . Options A and D might have some increase in complexity, but not necessarily a significant increase in degrees of freedom. Option C reduces degrees of freedom, making ΔS° negative.

Therefore, the correct answer is B.

Figure 15. The model displays an adeptness in processing chemistry.

Problem



Question: A furniture shop sells 3-seater, 2-seater and 1-seater sofas that each have an equally wide armrest on the left and the right hand side. Each seat is equally wide (see picture). Together with the armrests the 3-seater sofa is 220 cm wide and the 2-seater sofa 160 cm wide. How wide is the 1-seater sofa?

Choices:

- (A) 60 cm
- (B) 80 cm
- (C) 90 cm
- (D) 100 cm
- (E) 120 cm

Response

Okay, so I'm trying to figure out the width of the 1-seater sofa based on the information given. Let me start by understanding the problem.

We have three types of sofas: 3-seater, 2-seater, and 1-seater. Each has equally wide armrests on both sides, and each seat is equally wide. The total widths are given as 220 cm for the 3-seater and 160 cm for the 2-seater. We need to find the width of the 1-seater.

First, let's denote the width of each seat as (S) and the width of each armrest as (A) . Since there are two armrests per sofa, the total width of the sofa would be $(2A + 3S)$ for the 3-seater, $(2A + 2S)$ for the 2-seater, and $(2A + S)$ for the 1-seater.

From the image, we can see:

- The 3-seater sofa is 220 cm wide.
- The 2-seater sofa is 160 cm wide.

Using the image, we can set up the following equations:

1. For the 3-seater: $(2A + 3S = 220)$
2. For the 2-seater: $(2A + 2S = 160)$

We can solve these equations to find (A) and (S) .

Subtract the second equation from the first:

$$\begin{aligned} (2A + 3S) - (2A + 2S) &= 220 - 160 \\ (S) &= 60 \end{aligned}$$

Now, substitute $(S = 60)$ back into the second equation:

$$\begin{aligned} (2A + 2(60) &= 160) \\ (2A + 120 &= 160) \\ (2A &= 40) \\ (A &= 20) \end{aligned}$$

Now, we can find the width of the 1-seater sofa:

$$(2A + S = 2(20) + 60 = 40 + 60 = 100 \text{ cm})$$

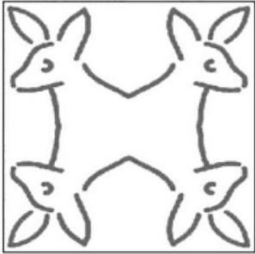
Therefore, the width of the 1-seater sofa is 100 cm .

The width of the 1-seater sofa is determined by calculating the individual seat and armrest widths using the given total widths of the 3-seater and 2-seater sofas. Solving the equations yields a seat width of 60 cm and an armrest width of 20 cm . Applying these to the 1-seater sofa gives a total width of 100 cm .

Answer: D

Figure 16. The model displays an adeptness in processing math.

Problem



Question: How many lines of symmetry does this figure have?

Response

The image shows a symmetrical design with two rabbits facing each other. Each rabbit has two lines of symmetry: one vertical and one horizontal. Since the rabbits are identical and arranged symmetrically, the entire figure has two lines of symmetry.

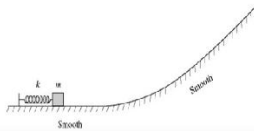
Therefore, the figure has 2 lines of symmetry.

The figure has 2 lines of symmetry.

Answer: 2

Figure 17. The model displays an adeptness in processing logic.

Problem



Question: A box of mass m is pressed against (but is not attached to) an ideal spring of force constant k and negligible mass. The spring is compressed a distance x . After it is released, the box slides up a frictionless incline as shown in the diagram at right and eventually stops. If we repeat this experiment with a box of mass $2m$

Choices:

- A. the lighter box will go twice as high up the incline as the heavier box.
- B. just as it moves free of the spring, the lighter box will be moving twice as fast as the heavier box.
- C. both boxes will have the same speed just as they move free of the spring.
- D. both boxes will reach the same maximum height on the incline.
- E. just as it moves free of the spring, the heavier box will have twice as much kinetic energy as the lighter box.

Response

Okay, so I'm trying to figure out this physics problem about a box being pushed against a spring and then released up an incline. Let me break it down step by step.

First, the setup: there's a box of mass (m) pressed against an ideal spring with force constant (k) . The spring is compressed by a distance (x) . When released, the box slides up a frictionless incline and stops. Then, the experiment is repeated with a box of mass $(2m)$. The question is asking which statement is correct regarding their behavior.

I remember that when a spring is compressed, it stores potential energy, which is converted into kinetic energy when released. The formula for the potential energy stored in a spring is $(\frac{1}{2}kx^2)$. So, when the spring is released, this energy becomes kinetic energy for the box.

Now, the box moves up an incline, which is frictionless, so all the kinetic energy turns into gravitational potential energy. The height (h) it reaches is given by $(mgh = \frac{1}{2}mv^2)$, where (v) is the initial velocity after the spring is released.

For the lighter box (m) , the initial kinetic energy is $(\frac{1}{2}kx^2)$. So, $(\frac{1}{2}kx^2 = \frac{1}{2}mv^2)$, which simplifies to $(v = \sqrt{\frac{kx^2}{m}})$. The height (h) it reaches is $(h = \frac{v^2}{2g} = \frac{\frac{kx^2}{m}}{2g} = \frac{kx^2}{2mg})$.

For the heavier box $(2m)$, the initial kinetic energy is $(\frac{1}{2}kx^2)$. So, $(\frac{1}{2}kx^2 = \frac{1}{2}(2m)v^2)$, which simplifies to $(v = \sqrt{\frac{kx^2}{2m}})$. The height (h) it reaches is $(h = \frac{v^2}{2g} = \frac{\frac{kx^2}{2m}}{2g} = \frac{kx^2}{4mg})$.

Comparing the heights, the lighter box reaches $(\frac{kx^2}{2mg})$ and the heavier box reaches $(\frac{kx^2}{4mg})$. So, the lighter box goes twice as high as the heavier box. That means option A is correct.

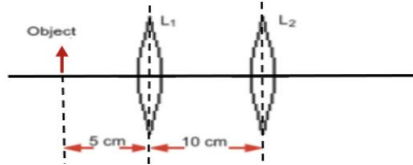
Alternatively, looking at the options:

- A. The lighter box goes twice as high as the heavier box. This matches my calculation.
- B. The lighter box moves twice as fast as the heavier box when released. The velocities are $(\sqrt{\frac{kx^2}{m}})$ and $(\sqrt{\frac{kx^2}{2m}})$, so the lighter box is moving faster, but not twice as fast.
- C. Both boxes have the same speed when released. No, their speeds are different.
- D. Both reach the same height. No, the heights are different.
- E. The heavier box has twice the kinetic energy. The kinetic energy is $(\frac{1}{2}mv^2)$, so for the lighter box, it's $(\frac{1}{2}m\left(\sqrt{\frac{kx^2}{m}}\right)^2 = \frac{1}{2}kx^2)$, and for the heavier box, it's $(\frac{1}{2}(2m)\left(\sqrt{\frac{kx^2}{2m}}\right)^2 = \frac{1}{2}kx^2)$. So both have the same kinetic energy, not twice as much.

So, the correct answer is A.

Figure 18. The model displays an adeptness in processing physical mechanics.

Problem



Question: A combination of two thin convex lenses is placed as shown at right. An object is placed 5 cm in front of L1 which has a focal length of 10 cm. L2 is 10 cm behind L1 and has a focal length of 12 cm. How far from L2 is the final image for this lens combination?

Choices:

- A. 8 cm
- B. 15 cm
- C. 22 cm
- D. 24 cm
- E. 30 cm

Response

Okay, so I'm trying to figure out how far the final image is from lens L2 in this setup. Let's start by analyzing the image itself. The image shows two convex lenses, L1 and L2, placed 10 cm apart. The object is 5 cm in front of L1, and L1 has a focal length of 10 cm. L2 is 10 cm behind L1 and has a focal length of 12 cm.

First, I need to determine the image distance for the first lens, L1. The object distance for L1 is 5 cm, and its focal length is 10 cm. Using the lens formula $\frac{1}{f} = \frac{1}{d_o} + \frac{1}{d_i}$:

$$\frac{1}{10} = \frac{1}{5} + \frac{1}{d_i}$$

Solving for (d_i) :

$$\frac{1}{d_i} = \frac{1}{10} - \frac{1}{5} = \frac{1}{10} - \frac{2}{10} = -\frac{1}{10}$$
$$[d_i = -10 \text{ cm}]$$

The negative sign indicates that the image is virtual and located 10 cm behind L1.

Next, the image from L1 is 10 cm from L1, and the object for L2 is 10 cm from L1, making the object distance for L2 20 cm. Using the lens formula for L2:

$$\frac{1}{12} = \frac{1}{20} + \frac{1}{d_i}$$

Solving for (d_i) :

$$\frac{1}{d_i} = \frac{1}{12} - \frac{1}{20} = \frac{5}{60} - \frac{3}{60} = \frac{2}{60} = \frac{1}{30}$$
$$[d_i = 30 \text{ cm}]$$

The positive sign indicates that the image is real and located 30 cm from L2.

Therefore, the final image is 30 cm from L2.

Answer: E

Figure 19. The model displays an adeptness in processing physical optics.

Problem

Substance	CH ₄ (g)	CH ₂ Cl ₂ (g)	HCl(g)
ΔH_f° , kJ·mol ⁻¹	-74.6	-95.4	-92.3

Question: $\text{CH}_4(\text{g}) + \text{Cl}_2(\text{g}) \rightarrow \text{CH}_2\text{Cl}_2(\text{g}) + 2\text{HCl}(\text{g})$. Use the data in the table below to calculate the standard enthalpy, ΔH° , for the reaction above.

Choices:

- A. -205 kJ·mol⁻¹
- B. -113 kJ·mol⁻¹
- C. 113 kJ·mol⁻¹
- D. 205 kJ·mol⁻¹

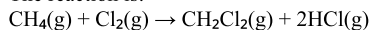
Response

Okay, so I need to calculate the standard enthalpy change, ΔH° , for the reaction $\text{CH}_4(\text{g}) + \text{Cl}_2(\text{g}) \rightarrow \text{CH}_2\text{Cl}_2(\text{g}) + 2\text{HCl}(\text{g})$. The table provides the standard enthalpies of formation (ΔH_f°) for each substance involved.

First, I'll identify the relevant ΔH_f° values from the table:

- CH₄(g) has $\Delta H_f^\circ = -74.6 \text{ kJ}\cdot\text{mol}^{-1}$
- Cl₂(g) has $\Delta H_f^\circ = 0 \text{ kJ}\cdot\text{mol}^{-1}$ (since it's a diatomic element in its standard state)
- CH₂Cl₂(g) has $\Delta H_f^\circ = -95.4 \text{ kJ}\cdot\text{mol}^{-1}$
- HCl(g) has $\Delta H_f^\circ = -92.3 \text{ kJ}\cdot\text{mol}^{-1}$

The reaction is:



To find ΔH° for this reaction, I need to calculate the difference between the sum of the products' ΔH_f° and the sum of the reactants' ΔH_f° .

So, the calculation is:

$$\Delta H^\circ = [\Delta H_f^\circ(\text{CH}_2\text{Cl}_2) + 2 \times \Delta H_f^\circ(\text{HCl})] - [\Delta H_f^\circ(\text{CH}_4) + \Delta H_f^\circ(\text{Cl}_2)]$$

Plugging in the values:

$$\Delta H^\circ = [-95.4 + 2 \times (-92.3)] - [-74.6 + 0]$$

$$\Delta H^\circ = [-95.4 - 184.6] - [-74.6]$$

$$\Delta H^\circ = -280 - (-74.6)$$

$$\Delta H^\circ = -280 + 74.6$$

$$\Delta H^\circ = -205.4 \text{ kJ}\cdot\text{mol}^{-1}$$

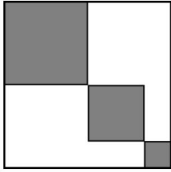
Rounding to one decimal place, $\Delta H^\circ \approx -205 \text{ kJ}\cdot\text{mol}^{-1}$.

Looking at the options, A is $-205 \text{ kJ}\cdot\text{mol}^{-1}$, which matches my calculation.

Answer: A

Figure 20. The model displays an adeptness in processing chemical reaction.

Problem



Question: In the diagram, a square with side length 6 is partially shaded. The largest shaded region is a square with side length 3. The other two shaded regions are squares with side lengths 2 and 1. What is the total area of the unshaded region?

Choices:

- A. 12
- B. 18
- C. 22
- D. 24
- E. 30

Response

The image shows a large square with a side length of 6 units, which has a total area of 36 square units. Inside this large square, there are three smaller shaded squares with side lengths of 3, 2, and 1 units. The areas of these shaded squares are 9, 4, and 1 square units respectively.

To find the total area of the unshaded region, we need to subtract the areas of the shaded squares from the total area of the large square. The total area of the shaded squares is $9 + 4 + 1 = 14$ square units. Therefore, the unshaded area is $36 - 14 = 22$ square units.

The total area of the unshaded region is 22 square units.

Answer: C

Figure 21. The model displays an adeptness in processing math geometry.

Problem

Volume of CO ₂ (number of bubbles)	Time taken for rennin to curdle milk samples (seconds)				
	Trial 1	Trial 2	Trial 3	Trial 4	Average
100	253	257	250	260	255
150	238	232	241	229	235
200	216	214	219	211	215
250	208	202	212	198	205
300	210	200	199	311	203

Question: Chymosin, known also as rennin, is a proteolytic enzyme related to pepsin that is synthesised by chief cells in the stomach of some animals. Its role in digestion is to curdle or coagulate milk in the stomach, a process of considerable importance in the very young animal. If milk were not coagulated, it would rapidly flow through the stomach and miss the opportunity for initial digestion of its proteins. Students investigated rennin activity. They bubbled different volumes of carbon dioxide (CO₂) gas into milk samples. Each sample was 50 mL and was kept at a constant temperature. The students then added rennin to each milk sample and recorded the time taken for the milk to curdle. What can the students conclude from the results of their rennin investigation?

Choices:

- A. Rennin does not curdle milk.
- B. The results are too varied to make any conclusion.
- C. The volume of carbon dioxide bubbled through the milk samples increases the time taken to curdle the milk.
- D. The volume of carbon dioxide bubbled through the milk samples decreases the time taken to curdle the milk.

Response

Okay, so I need to figure out what the students can conclude from their rennin investigation. Let me start by understanding the setup. They used different volumes of CO₂ gas in milk samples, each 50 mL, kept at a constant temperature. Then they added rennin and measured how long it took for the milk to curdle.

Looking at the data, the CO₂ volumes are 100, 150, 200, 250, and 300 bubbles. The times taken are in seconds, and the averages are given. The times decrease as the CO₂ volume increases. For example, 100 bubbles take about 255 seconds, 150 bubbles take 235, 200 bubbles take 215, 250 bubbles take 205, and 300 bubbles take 203 seconds.

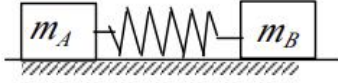
So, as the CO₂ volume increases, the time taken to curdle decreases. This suggests that more CO₂ leads to faster curdling. Since CO₂ is a gas, it might be affecting the milk's properties, maybe making it more acidic or changing its structure, which could speed up the rennin's action.

Therefore, the conclusion should be that the volume of CO₂ decreases the time taken to curdle the milk.

Answer: D

Figure 22. The model displays an adeptness in processing biology.

Problem



Question: The masses of two wooden blocks A and B are m_A and m_B respectively, with $m_B = 2m_A$. They are connected by a light spring and rest on a smooth horizontal table as shown in the figure. If an external force compresses the spring by pushing the two blocks closer and then the force is removed, the ratio of the kinetic energies of the two blocks in motion E_{KA}/E_{KB} is

Choices:

- A. $\frac{1}{2}$
- B. $\frac{\sqrt{2}}{2}$
- C. $\sqrt{2}$
- D. 2

Response

Okay, so I'm trying to solve this physics problem about two blocks connected by a spring on a smooth table. Let me break it down step by step.

First, the image shows two blocks, A and B, with masses (m_A) and (m_B) respectively. The image also shows that (m_B) is twice the mass of (m_A) , so $(m_B = 2m_A)$. They are connected by a light spring, which means the spring is massless and doesn't add any extra mass. The setup is on a smooth horizontal table, so there's no friction involved.

The problem states that an external force compresses the spring, bringing the two blocks closer together. Then, when the force is removed, the blocks start moving. We need to find the ratio of their kinetic energies, (E_{KA}/E_{KB}) .

When the external force is removed, the spring will exert forces on both blocks, causing them to move. Since the spring is light, the acceleration of each block will depend on their respective masses. According to Newton's second law, $(F = ma)$, so the acceleration (a) is (F/m) .

For block A, the force is (F) , so $(a_A = F/m_A)$. For block B, the force is also (F) , so $(a_B = F/m_B)$. Since $(m_B = 2m_A)$, $(a_B = F/(2m_A))$, which is half of (a_A) .

Now, kinetic energy is given by $(KE = \frac{1}{2}mv^2)$. Since both blocks start from rest and move under the same force, their velocities will depend on their accelerations. After some time, they will have velocities (v_A) and (v_B) .

The ratio of their kinetic energies is $(\frac{E_{KA}}{E_{KB}}) = \frac{\frac{1}{2}m_A v_A^2}{\frac{1}{2}m_B v_B^2} = \frac{m_A v_A^2}{m_B v_B^2}$.

Since $(a_A = \frac{F}{m_A})$ and $(a_B = \frac{F}{m_B})$, the ratio of their accelerations is $(\frac{a_A}{a_B} = \frac{m_B}{m_A} = 2)$. This means $(v_A = 2v_B)$.

Substituting $(v_A = 2v_B)$ into the kinetic energy ratio, we get:

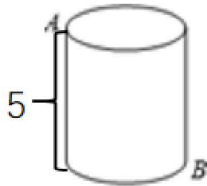
$$\left[\frac{E_{KA}}{E_{KB}} \right] = \frac{m_A (2v_B)^2}{m_B v_B^2} = \frac{m_A \cdot 4v_B^2}{m_B v_B^2} = \frac{4}{2} = 2$$

Therefore, the ratio of the kinetic energies is 2.

Answer: D

Figure 23. The model displays an adeptness in processing physical mechanics.

Problem



Question: As shown in the figure, a cylinder with a bottom circumference of 24.0, the shortest route that an ant passes along the surface from point A to point B is ()

Choices:

A: 12m

B: 15m

C: 13m

D: 14m

Response

Okay, so I'm trying to solve this problem about the shortest path an ant takes on a cylinder. The image shows a cylinder with a bottom circumference of 24.0 meters. Points A and B are on the surface, and the ant needs to find the shortest path from A to B.

First, I remember that when dealing with shortest paths on curved surfaces, sometimes it's helpful to unfold the cylinder into a flat shape. As seen in the image, if I imagine cutting the cylinder along a vertical line and laying it flat, the bottom becomes a rectangle. The height of this rectangle would be the height of the cylinder, which is 5 meters, and the width would be half the circumference because the ant can travel around the cylinder.

So, the rectangle would have a height of 5 meters and a width of 12 meters (since 24 divided by 2 is 12). Now, the shortest path on the cylinder should correspond to the straight line on this rectangle. To find the length of this straight line, I can use the Pythagorean theorem.

The theorem states that in a right-angled triangle, the square of the hypotenuse (which would be the shortest path here) is equal to the sum of the squares of the other two sides. So, if I let the shortest path be 'd', then:

$$d^2 = 5^2 + 12^2$$

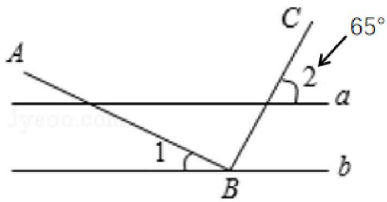
Calculating that, 5 squared is 25, and 12 squared is 144. Adding those together gives 169. Taking the square root of 169 gives me 13. So, the shortest path should be 13 meters.

Looking at the options provided, option C is 13 meters, so that must be the correct answer.

Answer: C

Figure 24. The model displays an adeptness in processing math.

Problem



Question: As shown in the figure, the straight line a parallel b , and AB perpendicular BC , then the degree of angle 1 is ()

Choices:

A: 65°

B: 25°

C: 35°

D: 45°

Response

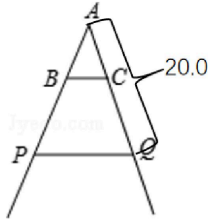
The image shows two parallel lines, a and b , intersected by a transversal. AB is perpendicular to BC , forming a right angle at B . Angle 2 is 65° , and angle 1 is adjacent to it. Since a and b are parallel, angle 2 and its corresponding angle on line b are equal. Thus, the angle adjacent to angle 1 is 65° . As AB is perpendicular to BC , angle 1 is $90^\circ - 65^\circ = 25^\circ$.

Therefore, the measure of angle 1 is 25° , which corresponds to option B.

Answer: B

Figure 25. The model displays an adeptness in processing math.

Problem



Question: It is known that BC parallel PQ, $AB:AP = 2.0:5.0$, then the length of CQ is ()

Choices:

- A:8cm
- B:12cm
- C:30cm
- D:50cm

Response

Okay, so I'm trying to solve this geometry problem where BC is parallel to PQ, and the ratio of AB to AP is 2:5. I need to find the length of CQ. The image shows a triangle with points A, B, C, P, and Q. BC is parallel to PQ, which means that triangles ABC and APQ are similar because of the parallel lines.

Since BC is parallel to PQ, the triangles ABC and APQ are similar by the Basic Proportionality Theorem (Thales' theorem).

This theorem states that if a line is drawn parallel to one side of a triangle, it divides the other two sides proportionally.

The ratio of AB to AP is given as 2:5. This means that AB is 2 parts and AP is 5 parts. Since the triangles are similar, the ratio of their corresponding sides should be the same. Therefore, the ratio of BC to PQ should also be 2:5.

The image shows that PQ is 20 cm. Using the ratio, we can set up the proportion:

$$\frac{BC}{PQ} = \frac{2}{5}$$

Substituting $PQ = 20$ cm into the proportion:

$$\frac{BC}{20} = \frac{2}{5}$$

Solving for BC:

$$BC = \frac{2}{5} \times 20 = 8 \text{ cm}$$

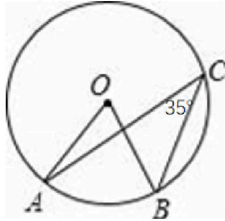
Since BC is parallel to PQ, the length of CQ is the remaining part of PQ after subtracting BC. Therefore, $CQ = PQ - BC = 20 - 8 = 12$ cm.

So, the length of CQ is 12 cm, which corresponds to option B.

Answer: B

Figure 26. The model displays an adeptness in processing math.

Problem



Question: As shown in the figure, O is the center of the circle, then the degree of angle AOB is ()

Choices:

A: 35°

B: 70°

C: 105°

D: 150

Response

Okay, so I'm trying to solve this geometry problem where I need to find the measure of angle AOB in a circle. The image shows a circle with center O, and points A, B, and C on the circumference. The angle at point C, which is angle ACB, is given as 35 degrees. The question is asking for the measure of angle AOB.

Hmm, I remember something about angles in circles. There's a theorem that relates central angles to inscribed angles. Let me think... Oh right! The Inscribed Angle Theorem states that an inscribed angle is half the measure of the central angle that subtends the same arc. So, if angle ACB is an inscribed angle, then the central angle AOB should be twice that.

So, if angle ACB is 35 degrees, then angle AOB should be 2 times 35 degrees. Let me calculate that: 2 multiplied by 35 is 70 degrees. That makes sense because the central angle is always larger than the inscribed angle for the same arc.

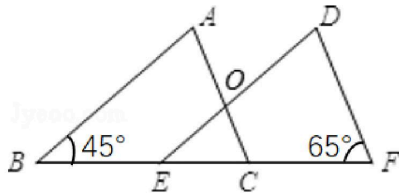
Looking at the choices provided: A is 35° , B is 70° , C is 105° , and D is 150° . So, 70° is option B. That must be the correct answer.

I don't think I made any mistakes here. The key was remembering the Inscribed Angle Theorem and applying it correctly. So, yeah, angle AOB is 70 degrees.

Answer: B

Figure 27. The model displays an adeptness in processing math geometry.

Problem



Question: As shown in the figure, triangle ABC congruent triangle DEF, then the degree of angle COE is ()

Choices:

A:40°

B:60°

C:70°

D:100

Response

Okay, so I'm trying to solve this geometry problem where triangle ABC is congruent to triangle DEF. The question is asking for the measure of angle COE. The image shows that angle B is 45 degrees and angle F is 65 degrees. Since the triangles are congruent, their corresponding angles are equal. Therefore, angle A in triangle ABC corresponds to angle D in triangle DEF, angle B corresponds to angle E, and angle C corresponds to angle F.

Given that angle B is 45 degrees, angle E must also be 45 degrees. Similarly, since angle F is 65 degrees, angle C must also be 65 degrees. Now, angle COE is the angle at point O between points C and E. As seen in the image, angle COE is formed by the intersection of lines CO and EO, which are the extensions of sides AC and DF respectively.

Since angle C is 65 degrees and angle E is 45 degrees, and they are adjacent angles forming a linear pair, their sum is 180 degrees. Therefore, angle COE, which is the remaining angle, is $180 - 65 - 45 = 70$ degrees.

Thus, the measure of angle COE is 70 degrees.

Answer: C

Figure 28. The model displays an adeptness in processing math geometry.